Self-Assembled Organic Crystalline Microrings as Active Whispering-Gallery-Mode Optical Resonators

Chuang Zhang, Chang-Ling Zou, Yongli Yan, Cong Wei, Jin-Ming Cui, Fang-Wen Sun, Jiannian Yao, and Yong Sheng Zhao**

Light confinement within micro/nanoscale volumes allows a profound engineering of light-matter interactions to realize nanophotonic components for all-optical signal processing.[1–3] High quality nanowires can travel light forth and back, and serve as Fabry-Pérot (FP) resonators to enhance optical gains for light amplification.[4–6] The major drawback of such nanowire cavities is their low reflectivity at end facets,[7] which implies most of traveled photons are outcoupled from cavities at wire tips. One simple yet effective solution is to join the two ends of a nanowire into a pseudo-ring conformation,[8,9] where the light might be better confined via the formation of whispering gallery mode (WGM) resonance.[10] Practical applications of these artificial optical geometries are still hindered for their inconvenient fabrication and the unexpected light scattering and energy leakage at joint points.

The chemical versatility and flexible nature of organic materials allow for numerous kinds of micro/nano-assemblies,[11–13] even highly bent ones as tubes,[14] twists,[15] and also rings.[16,17] These self-assembled molecular micro/nanocrystals have been already applied in multiple nanophotonic units, including nanolasers,[18] optical routers,[19] modulators,[20] sensors[21] and logic gates.[22] However, the construction of active WGM ring resonators,[23] as a kind of fundamental photonic units, is still a challenge, because self-assembled rings often suffer from a low structural quality of optical defects or a tiny size below diffraction limits.[24] In this paper, we propose an improved self-assembly strategy in microscopic solution droplets to produce organic crystalline microrings with high structural quality, in which optical WGM resonance of fluorescence could efficiently occur. These self-assembled WGM resonators would take advantages of facile preparation, active optical responses, free of mechanical defects and well-defined circular shapes, offering great potentials in low-threshold WGM microlasers,[25] interferometers,[26] optical sensors,[27] wavelength filters[28] and slow-light devices.[29]

C. Zhang, Dr. Y. Yan, C. Wei, Prof. J. Yao, Prof. Y. S. Zhao
Beijing National Laboratory for Molecular Sciences (BNLMS)
Key Laboratory of Photochemistry
Institute of Chemistry
Chinese Academy of Sciences (ICCAS)
Beijing, 100190, China
Tel: (+) 86–10–62652029; Fax: (+) 86–10–62652029
E-mail: jnyao@iccas.ac.cn; yszhao@iccas.ac.cn
C.-L. Zou, J.-M. Cui, Prof. F.-W. Sun
Key Laboratory of Quantum Information
University of Science and Technology of China
(USTC), Hefei, Anhui, 230026, China

DOI: 10.1002/adom.201200065

The crystal of organic compound 1,5-diphenyl-1,4-pentadien-3-one (DPPDO) (**Figure 1**a), where molecules can be rearranged in the loose crystal lattice, was adopted due to its good tolerance for structural distortions.[30] Here, we realized the circular growth of DPPDO microcrystals by introducing the liquid tension of solution droplets during the process of molecular assembly. The final configuration and size of DPPDO assemblies could be easily controlled by changing the concentration of molecules in solution. In the as-prepared microrings, the fluorescence emission could be efficiently guided and locally confined, resulting in WGM spectral modulation of the outcoupled light signals. The quality (Q) factor of these self-assembled WGM resonators could exceed 300, which means the better confinement of photons and stronger exciton-photon coupling over those in nanowires FP cavities.[10,31]

When DPPDO molecules were dissolved in a mixed solvent of ethanol/water (volume ratio = 1/20) and then kept undisturbed for hours, they could aggregate into crystalline microbelts as shown in Figure 1b. These molecular assemblies grew along the [001] crystal direction, as indicated in the corresponding selected area electron diffraction (SAED) patterns. The molecular planes are perpendicular to the c axis and have a large space between neighboring molecules, which means that the c parameter has a considerably variable range within the tolerance of weak intermolecular interactions. As a result, the self-assembled DPPDO belts are of remarkable flexibility (Figure S1), which implies the bendable molecular packing in the preferential growth direction.[17,32] It is very possible to achieve self-assembled microring structures from the aggregation of DPPDO molecules, as long as an appropriate driven force could be applied for the circular growth during the assembly process.

An efficient route to ring formation is to use the essential contact lines around evaporating liquid drops on a solid substrate.[33,34] Inspired by this, we could realize the circular assembly of DPPDO (Inset in Figure 1c), when its ethanol/water solution was freshly mixed and drop-cast on a glass slide (See Experimental Section for details). After the complete evaporation of solvent, well-defined ring-like structures with a uniform diameter were observed on substrate, as displayed in Figure 1c. The SEM image (Figure 1d) illustrates a relative smooth surface of these rings, and also their flexibility oriented to the$b$ crystal axis due to the considerable height to width (h/w) ratio (Inset in Figure 1d). These results indicated that the rings are formed from the bent growth of belts, induced by the liquid tension in hemispherical-shaped microdroplets during the evaporation (Figure S2). The phase difference inside and outside the microdroplets provide an anisotropic environment for ring formation to occur rather than the unrestricted one-dimensional aggregation in homogeneous solution.[31,35]

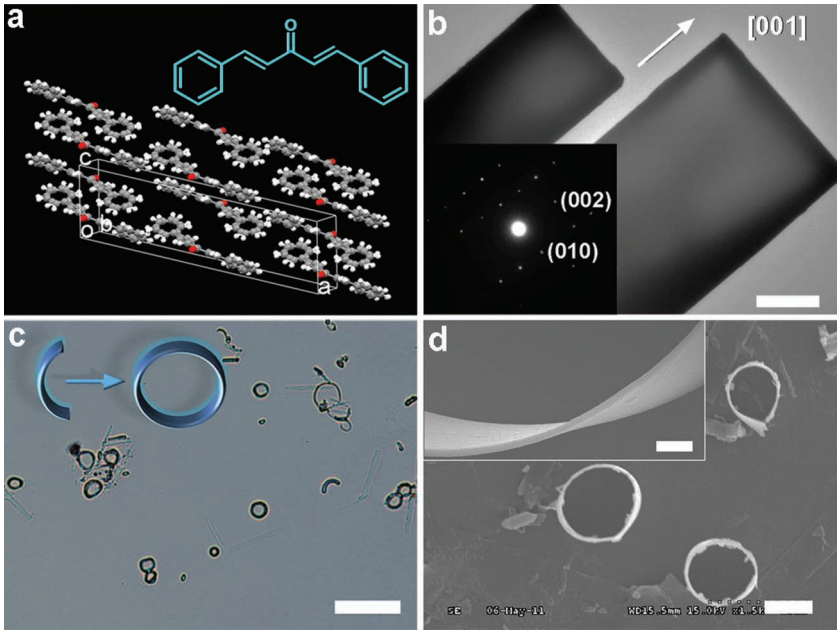

Figure 1. (a) Molecular packing in a DPPDO crystal with probable lattice distortions. Inset: molecular structure of DPPDO. (b) TEM image of self-assembled DPPDO microbelts. Scale bar is 1 μm. Inset: SAED pattern of a single belt. (c) Large-scale optical microscopy image of the as-prepared DPPDO assemblies on glass substrate. Scale bar is 50 μm. Inset: illustration of the circular growth driven by liquid tension. (d) SEM image of several separated microrings. Scale bar is 10 μm. Inset: high-resolution SEM image of the bent part of a typical ring. Scale bar is 2 μm.

By combining the above morphological results, we propose an optimized model for the ring formation process driven by interfacial tension,[36] as illustrated **Figure 2**a. In a microsized droplet of mixed solution on the glass substrate, DPPDO should nucleate preferentially at the contact line, where the solvent evaporated faster than that in the central area. The solution droplet was therefore confined within the inner surface, and offered a circular template for the assembly around the droplet. Then, the molecular units aggregated with a larger *c* parameter at the outer surface, because the direction of molecular packing was bent by the force of liquid tension at the contact line. With the further evaporation of solvent, the assemblies could grow into a curved belt that embraced the microdroplet. Moreover, the defects between curved blocks could be filled by molecules in the solution droplet via the weak intermolecular interaction. As a result, self-assembled microrings without noticeable defects or joints were finally obtained after the exhaustion of DPPDO molecules in the evaporating droplets.

From the growth model described above, we can see that the rate and time period of molecular aggregation should be strongly dependent on the amount of DPPDO units in the microdroplets. Thereby, the molar concentration of drop-casting solutions could determine the morphological parameters (e.g., dimension, curvature and size) of the final structures. When the concentration is 2 mmol L^{-1}, the insufficient growth resulted in only wire-like structures, which are too short to be bent and connected into rings (Figure 2b). Although these wires might be slightly bent at the beginning of assembly period, they were more likely to unfold into straight ones after the evaporation due to their low length to diameter ratio. When a solution with a concentration of 4 mmol L^{-1} was adopted, longer warped belts and microrings with a diameter of ~5 μm were observed on substrate, as shown in Figure 2c. It indicates that 4 mmolL^{-1} is the critical concentration that allows for ring formation just before the termination stage. Therefore, rings with a larger diameter would be prepared in solutions with a higher concentration, because they can formed at an earlier stage when the evaporating droplet was still of a larger volume. As expected, the perfect circular conformation (~10 μm) was prepared from a 6 mmol L^{-1} solution, as displayed in Figure 2d. However, only microtiles of tens of micrometers (Figure 2e) were obtained at a further increased concentration of 10 mmol L^{-1}, because the molecular aggregation became too fast, and also brought too large mechanical resistance to assemble crystalline nucleus into circular structures.

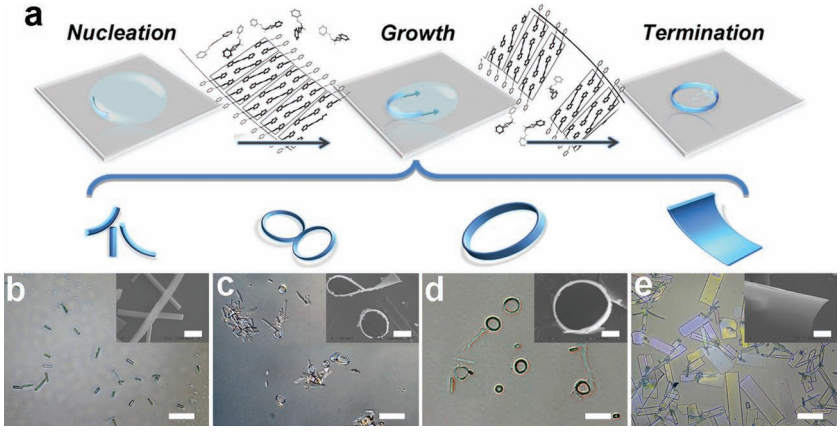

Figure 2. (a) Illustration of the formation mechanism of the self-assembled microrings driven by the interfacial tension of liquid droplets. By this means, typical products (wires, rings, tiles) could be obtained by controlling the solution concentration. (b-e) Optical microscopy images of wires, small/large rings and tiles obtained by using DPPDO solutions with different concentrations of 2 mmol L^{-1}, 4 mmol L^{-1}, 6 mmol L^{-1} and 10 mmol L^{-1}. Scale bars are 25 μm. Insets: corresponding SEM images. Scale bars are 2 μm.

The microsized assemblies of DPPDO molecules emitted instinct blue fluorescence under UV excitation via radiative transition of π-electrons, as shown in **Figure 3**a. The uniform light emission indicates that DPPDO structures are free of optical defects, which implies their potential abilities of optical waveguide and spatial confinement of fluorescent photons.[6,18] When DPPDO belts were excited locally by a focused UV laser

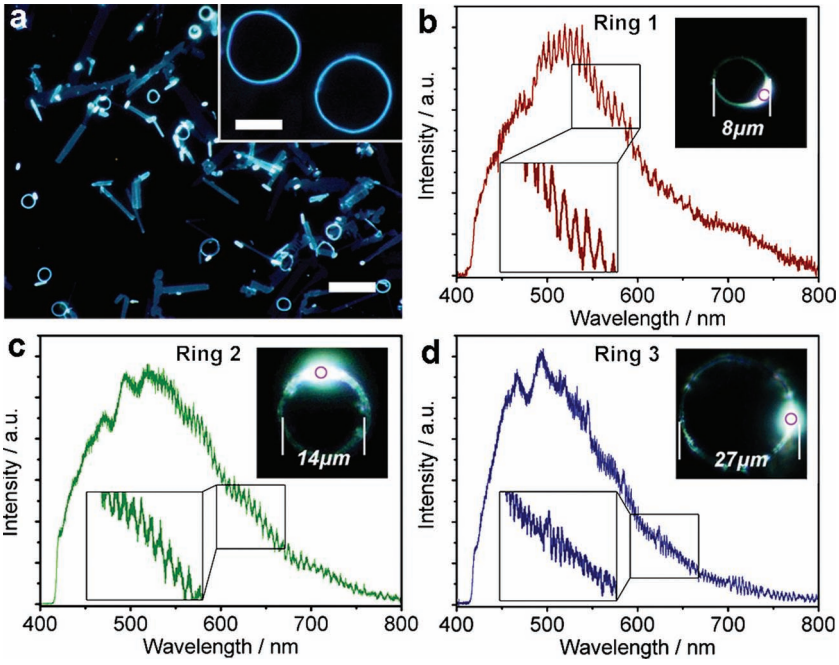

Figure 3. (a) Fluorescence microscopy image of the as-prepared DPPDO microstructures excited with UV band (330-380 nm) of a mercury lamp. Scale bar is 50 μm. Inset: high-magnification image of the DPPDO microrings. Scale bar is 10 μm. (b–d) Spatially resolved spectra outcoupled from DPPDO microrings with diameters of 8 μm, 14 μm, and 27 μm. Insets: fluorescence microscopy image of the microrings locally excited with a focused 351 nm laser beam. The excitation positions are marked with the violet circles, and the spectra were collected from the unexcited areas.

beam, light flows could be steered from the excitation spot towards tips (Figure S3). The outcoupled spectra revealed little loss occurs at the curved area, which could be attributed to active optical waveguide mode of fluorescence.[2,31] Most of the emitted photons were outcoupled at the low reflective end facets,[7] so that no FP type spectral modulation could be detected from the wire geometries. Nevertheless, in the DPPDO microring waveguides, the light emission could travel around and be trapped in the optical modes without outcoupling at end facets.[8] As displayed in the fluorescence images (Insets in Figure 3b–d), the fluorescence was waveguided and observed from the entire rings although the samples were locally excited by a laser beam. In these ring cavities with central symmetrical shapes and rather small sizes, the propagated photons were thereby trapped to generate WGM optical resonance at the circular boundary.[10]

A series of sharp peaks from the WGM modulation was found over the emission band in the outcoupled spectra, as shown in Figure 3b–d. In this optical active structure, the modes emerge more obviously at the range from 500 nm to 700 nm, because of the strong re-absorption of higher energy photons at shorter wavelength and the low optical gain at longer wavelength regions.[18,31] The mode spacing between the peaks decreases rapidly with an increase in ring diameter from 8 μm to 14 μm, and to 27 μm. It should be noted that such optical modulation was not observed at the excitation spots (Figure S4), where most of emitted photons are from the unguided light scattering rather than the light outcoupling of ring cavities. It indicates that the optical modulation is based on the confinement of photons within the rings, and thus, the rings function as optical WGM resonators of fluorescence. These assembled rings were perfectly connected without joint points, and the backscattering was therefore minimized to improve the degeneracy of clockwise and anticlockwise light propagation. The breakdown of spectral degeneracy should be quite limited compared with the line width of ring modes, so we did not observe notable peak splitting into doublets which is a common drawback in mechanically joined pseudo-rings.[8,10]

The optical modulation of WGM resonance in these organic rings could be better analyzed by removing the fluorescent background, as shown in **Figure 4**a. For instance, the spacing between peaks is 5.8 nm, 2.6 nm

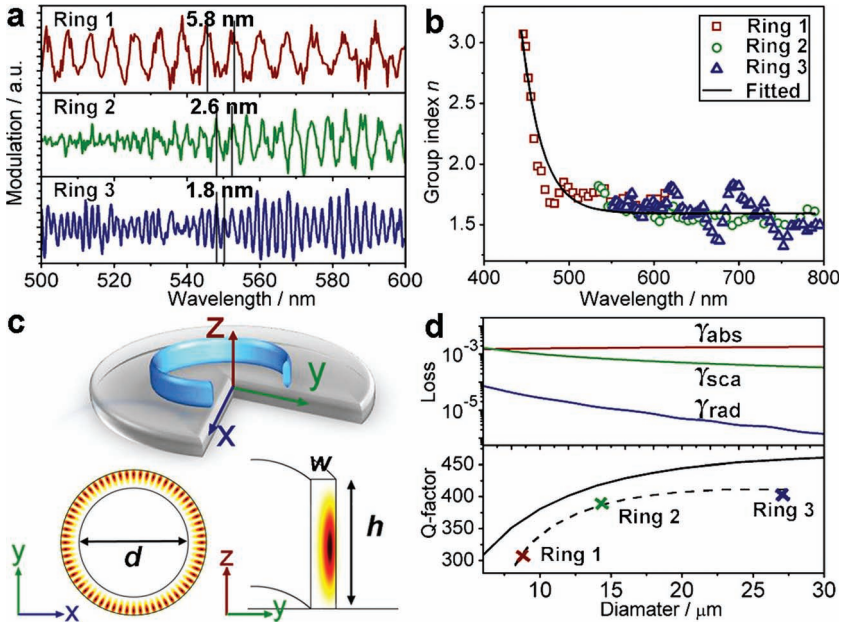

Figure 4. (a) WGM modulation within the range of 500–600 nm in rings 1–3 by removing the fluorescence background. (b) The plots and fitted curve of group index versus wavelength in these microrings. (c) Simulated 3D electric field intensity distribution (λ = 550 nm, n = 1.60) in the microring resonator (d = 4 μm, w = 500 nm, h = 3 μm). (d) The curves of estimated optical losses (absorption, scattering, and radiation) and total Q factor versus ring diameter. The dashed line was fitted from the experimental Q factors in rings 1–3.

and 1.8 nm at 550 nm for rings 1, 2 and 3, respectively. The spacing between the spectral peaks $\Delta\lambda$ is given by $\Delta\lambda = \lambda^2/n\pi d$, where λ is the wavelength of guided light, n is the group refractive index, and d is the diameter of ring.[10] The value of $\Delta\lambda$ exhibits a quadratic growth with the emission wavelengthλ, and is in inverse proportion to the optical path length $n\pi d$. Therefore, the group index n could be calculated to profile the optical dispersion relations in active microring cavities, as plotted in Figure 4b. The n value shows a curve that dramatically decreases with the increase of wavelength at the region below 550 nm, and then reaches a stable value (~1.60), which is identical in all the three microrings with different sizes. The dispersion curve indicates efficient exciton-photon coupling at the high-energy band of photons, which may help to explain the results that the resonance at short wavelength is more obvious in rings with a smaller size.

Three-dimensional (3D) local electric field distribution within microring structures was numerically simulated with finite element method, which profiles the circular interference of confined light as typical WGM resonance, as displayed in Figure 4c. It is noticeable that the electric field of light is almost localized at the outer half of the ring, indicating the photons are trapped by the total reflection at the outer interface between ring and air. The electric field on the x-y equatorial plane shows a distribution of periodic patterns in the azimuth direction, and the number of nodes increased linearly with the ring diameter (Figure S5). The profile of cross-section (y-z plane) reveals that the traveled light could be totally confined due to the high h/w ratio of microrings, although the refractive index of organic dielectric is close to that of the glass substrate.[18] The energy leakage to substrate can be ignored; however, the intensity distribution of light shows a curvature-dependent bias to the outer surface of ring (Figure S6), resulting in the optical leakage of confined photons during the circular propagation of photons.

There are three major sources of optical losses, light absorption, surface scattering and radiation,[9] that should be involved in these active WGM resonators, as illustrated in Figure 4d. The absorption loss γ_{abs} keeps unchanged with the ring circumference, because the absorption coefficient of DPPDO molecules is constant at a given wavelength (Figure S7). The scattering loss γ_{sca} is mainly caused by the roughness of the outer surface of rings, and the scattering intensity decreases in the ring with a large volume due to the better confinement of photons. The radiation loss γ_{rad} is the photon tunneling out of cavities on the surface evanescent wave, and shows an exponential decline with the ring diameter. The inverse of the sum of above-mentioned three kinds of optical losses, $1 / (\gamma_{abs} + \gamma_{sca} + \gamma_{rad})$, was calculated to estimate the quality of cavities.[37] The estimated curve of Q factor drastically increases from 300 to 400 with the increase of ring diameter, and gradually reaches a saturation region (~450) beyond a ring size of 20 μm. It agrees well with the variation of experimental Q factors in rings, which only decrease slightly due to the uncertainties in actual losses.

In conclusion, the crystalline dielectric microrings were prepared from small organic molecules DPPDO via a liquid-phase self-assembly approach, by inducing the crystal growth with the liquid tension of droplets on substrates. The microdroplets served as soft templates, and enabled facile control on the morphology and size of obtained structures. The assembled microring could well confine its fluorescence as active WGM resonance. The coupling between excitons and photons drastically altered the optical dispersion relations in the organic microring. The self-assembled microring cavity has a Q factor over 300, offering considerable potentials in active photonic components with spectral modulation abilities and compact sizes. There is still plenty of space for the improvements of luminescent efficiency and structural quality in the assembled rings. Therefore, we believe our demonstration of self-assembled WGM microring resonators would pave a new road to the extensive exploration of organic active components for integrated photonics.

Experimental Section

Materials: Organic compound 1,5-diphenyl-1,4-pentadien-3-one (DPPDO) was purchased from Meryer (Shanghai) Chemical Technology Co. Ltd., and used without further treatment. Ethanol (HPLC grade) was obtained from Beijing Chemical Agent Inc., and used without further purification. Ultrapure water with a resistivity of 18.2 MΩ cm was produced using a Milli-Q apparatus (Millipore).

Procedure: Organic microrings were prepared through a self-assembly method by drop-casting solution on a solid substrate. In a typical preparation, a stock solution of DPPDO (500 μL) in ethanol was rapidly injected into a tube of ultrapure water (10 mL) at ice-water bath condition. Then the tube was kept for 30 min at 0 °C to achieve intensive mixing of solvents without obvious precipitation. After that, a drop of as-prepared mixed solution (50 μL) was cast onto a glass slide, and left without any disturbance at room temperature for 3 h. The evaporation of surrounding solvents can induce the aggregation and assembly of DPPDO molecules. Finally, self-assembled microrings were obtained on substrate after the solvents completely evaporated.

Characterization: The morphology and crystallinity of DPPDO microstructures were examined by scanning electron microscopy (SEM, Hitachi S-4300) and transmission electron microscopy (TEM, JEOL JEM-1011). The absorption and fluorescence spectra were measured on a UV-visible spectrometer (Perkin-Elmer Lambda 35) and a fluorescent spectrometer (Hitachi F-7000), respectively. Bright-field optical images and fluorescence microscopy images were taken from an inverted fluorescence microscope (Nikon Ti-U), by exciting the samples with the UV band (330–380 nm) of a mercury lamp. The single microbelts and microrings were locally excited by a focused 351 nm Ar ion laser beam (Spectra-Physics Beamlok, spot size 2 μm). The spatially resolved spectra were measured with a monochrometer (Princeton Instrument Acton SP 2300i) connected with an EMCCD (Princeton Instrument ProEM 1600B).

Supporting Information

Supporting Information is available from the Wiley Online Library or from the author.

Acknowledgements

This work was supported by the National Natural Science Foundation of China (Nos. 21125315, 91022022, 51073164), the Chinese Academy of Sciences, and the Ministry of Science and Technology of China (2012YQ120060 and National Basic Research 973 Program).

Received: December 4, 2012
Revised: February 8, 2013
Published online: April 2, 2013

[1] M. Law, D. J. Sirbuly, J. C. Johnson, J. Goldberger, R. J. Saykally, P. D. Yang, *Science* **2004**, *305*, 1269.
[2] C. J. Barrelet, A. B. Greytak, C. M. Lieber, *Nano Lett.* **2004**, *4*, 1981.
[3] B. Piccione, C.-H. Cho, L. K. van Vugt, R. Agarwal, *Nat. Nanotechnol.* **2012**, *7*, 640.
[4] M. H. Huang, S. Mao, H. Feick, H. Q. Yan, Y. Y. Wu, H. Kind, E. Weber, R. Russo, P. D. Yang, *Science* **2001**, *292*, 1897.
[5] X. F. Duan, Y. Huang, R. Agarwal, C. M. Lieber, *Nature* **2003**, *421*, 241.
[6] D. O'Carroll, I. Lieberwirth, G. Redmond, *Nat. Nanotechnol.* **2007**, *2*, 180.
[7] S. Wang, Z. Hu, H. Yu, W. Fang, M. Qiu, L. Tong, *Opt. Express* **2009**, *17*, 10881.
[8] P. J. Pauzauskie, D. J. Sirbuly, P. D. Yang, *Phys. Rev. Lett.* **2006**, *96*, 143903.
[9] K. Takazawa, J.-i. Inoue, K. Mitsuishi, T. Takamasu, *Adv. Mater.* **2011**, *23*, 3659.
[10] R.-M. Ma, X.-L. Wei, L. Dai, S.-F. Liu, T. Chen, S. Yue, Z. Li, Q. Chen, G. G. Qin, *Nano Lett.* **2009**, *9*, 2697.
[11] L. Zang, Y. K. Che, J. S. Moore, *Acc. Chem. Res.* **2008**, *41*, 1596.
[12] Y. S. Zhao, H. B. Fu, A. D. Peng, Y. Ma, Q. Liao, J. Yao, *Acc. Chem. Res.* **2010**, *43*, 409.
[13] R. J. Li, W. P. Hu, Y. Q. Liu, D. B. Zhu, *Acc. Chem. Res.* **2010**, *43*, 529.
[14] Y. S. Zhao, J. J. Xu, A. D. Peng, H. B. Fu, Y. Ma, L. Jiang, J. Yao, *Angew. Chem. Int. Ed.* **2008**, *47*, 7301.
[15] T. Lei, H.-B. Chen, J. Yin, S. Huang, X. Zhu, J. Pei, *Org. Electron.* **2011**, *12*, 453.
[16] C. Jeukens, M. C. Lensen, F. J. P. Wijnen, J. Elemans, P. C. M. Christianen, A. E. Rowan, J. W. Gerritsen, R. J. M. Nolte, J. C. Maan, *Nano Lett.* **2004**, *4*, 1401.
[17] F. Balzer, J. Beermann, S. I. Bozhevolnyi, A. C. Simonsen, H. G. Rubahn, *Nano Lett.* **2003**, *3*, 1311.
[18] C. Zhang, C.-L. Zou, Y. Yan, R. Hao, F.-W. Sun, Z.-F. Han, Y. S. Zhao, J. Yao, *J. Am. Chem. Soc.* **2011**, *133*, 7276.
[19] J. Y. Zheng, Y. Yan, X. Wang, Y. S. Zhao, J. Huang, J. Yao, *J. Am. Chem. Soc.* **2012**, *134*, 2880.
[20] Q. L. Bao, B. M. Goh, B. Yan, T. Yu, Z. A. Shen, K. P. Loh, *Adv. Mater.* **2010**, *22*, 3661.
[21] J. Y. Zheng, Y. Yan, X. Wang, W. Shi, H. Ma, Y. S. Zhao, J. Yao, *Adv. Mater.* **2012**, *24*, OP194.
[22] Y. Yan, C. Zhang, J. Y. Zheng, J. Yao, Y. S. Zhao, *Adv. Mater.* **2012**, *24*, 5681.
[23] S. Fujiwara, K. Bando, Y. Masumoto, F. Sasaki, S. Kobayashi, S. Haraichi, S. Hotta, *Appl. Phys. Lett.* **2007**, *91*, 021104.
[24] N. Chandrasekhar, R. Chandrasekar, *Angew. Chem. Int. Ed.* **2012**, *51*, 3556.
[25] X.-F. Jiang, Y.-F. Xiao, C.-L. Zou, L. He, C.-H. Dong, B.-B. Li, Y. Li, F.-W. Sun, L. Yang, Q. Gong, *Adv. Mater.* **2012**, *24*, OP260.
[26] K. Takazawa, J.-i. Inoue, K. Mitsuishi, T. Kuroda, *Adv. Funct. Mater.* **2013**, *23*, 839.
[27] H. Li, L. Shang, X. Tu, L. Liu, L. Xu, *J. Am. Chem. Soc.* **2009**, *131*, 16612.
[28] H. Rokhsari, K. J. Vahala, *Phys. Rev. Lett.* **2004**, *92*, 253905.
[29] F. Xia, L. Sekaric, Y. Vlasov, *Nat. Photonics* **2007**, *1*, 65.
[30] I. Turowska-Tyrk, *Chem. Phys.* **2003**, *288*, 241.
[31] K. Takazawa, J. Inoue, K. Mitsuishi, T. Takamasu, *Phys. Rev. Lett.* **2010**, *105*, 067401.
[32] X. Y. Kong, Y. Ding, R. Yang, Z. L. Wang, *Science* **2004**, *303*, 1348.
[33] A. P. H. J. Schenning, F. B. G. Benneker, H. P. M. Geurts, X. Y. Liu, R. J. M. Nolte, *J. Am. Chem. Soc.* **1996**, *118*, 8549.
[34] R. D. Deegan, O. Bakajin, T. F. Dupont, G. Huber, S. R. Nagel, T. A. Witten, *Nature* **1997**, *389*, 827.
[35] K. Takazawa, *Chem. Mater.* **2007**, *19*, 5293.
[36] H.-D. Wu, Y. Xiao, G.-B. Pan, *Chem. Phys. Lett.* **2012**, *549*, 58.
[37] M. L. Gorodetsky, A. A. Savchenkov, V. S. Ilchenko, *Opt. Lett.* **1996**, *21*, 453.